STM JOURNALS

Journal of
Polymer & Composites

ISSN: 2321-2810 (Online)
ISSN: 2321-8525 (Print)
Volume 11, Special Issue 12, 2023
DOI (Journal): 10.37591/JoPC

http://engineeringjournals.stmjournals.in/index.php/JoPC/index

Research JoPC

Prediction of Temperatures and Residual Stresses During FSW of AA2024 and AA7075 with Copper Using Hyperweld Software

Pradeep Kumar Mouria[1,2*], Ranganath M. Singari[3], Reeta Wattal[4]

Abstract

This paper investigates the temperature at different workpiece and tool pin sections. In this investigation, various materials are utilized, for example, AA7050, AA2024, and Copper, for other process parameters. Tool rotational speed, tool tilt angle, and welding speed are process parameters. Thermal distribution results are examined with the assistance of these process parameters. Altair's Hyper Weld, a preeminent computer-aided engineering (CAE) application for the simulation of friction stir welding, has been used for detailed investigations. The outcomes are introduced for divergence in the top temperature of these distinctive aluminum and copper compound plates at similar information parameters during the Friction Stir Welding (FSW) process. It is observed that more heat is generated when the copper plate is placed on the right side, and the aluminum plate is placed on the left side.

Keywords: FSW, Peak temperature, AA7050, AA2024, copper, hyper weld.

INTRODUCTION

FSW (friction stir welding) is one of the famous solid state weldings for joining dissimilar materials. Friction stir welding is a new welding innovation by Wayne Thomas in 1991 at TWI in the UK. [1]. In FSW, a non-consumable tool is used, and as there is no production of fumes and spatter, there is also no need for filler material or shielding gases. That's why it does not harm the environment. The welding process has been done in three fundamental stages: Plunge, Dwell, and Translation [2]. Plunge is the primary phase of FSW; in this progression, the tool is rotated, and the tip is embedded into the workpiece. The shoulder surface is in contact with the two workpieces that will weld. During the welding process, a lot of heat is generated due to friction between the surface of the workpiece and the tool shoulder. This heat is sufficient to soften the region near the FSW tool, and as the tool is rotating, plastic movement and deformation of the material from the advanced side to the retreated side take place by the development of joints behind the motion of the tool. In the dwell step, the device rotates at a given rotational speed and is inserted into the plate at a particular location. The tool dwelled for some time to soften the material of the container. In the translation step, the device moves forward by joining the two plates. It was observed from the literature that 2XXX and 7XXX grades of aluminum have very high strength

Friction stir welding was used to join different grades of aluminum; some authors took AA7075 as the works piece [3–7]. Much research has been done on the FSW lap joint. It was observed that

***Author for Correspondence**
Pradeep Kumar Mouria

[1]Assistant Professor, Department of Mechanical Engineering, Manav Rachna University, Faridabad, Haryana, India
[2]Research Scholar, Department of Mechanical Engineering, Delhi Technological University, Delhi, India
[3]Professor, Department of Mechanical Engineering, Delhi Technological University, Delhi, India
[4]Professor, Department of Mechanical Engineering, Delhi Technological University, Delhi, India

Received Date: October 30, 2023
Accepted Date: December 20, 2023
Published Date: February 26, 2024

Citation: Pradeep Kumar Mouria, Ranganath M. Singari, Reeta Wattal. Prediction of Temperatures and Residual Stresses During FSW of AA2024 and AA7075 with Copper Using Hyperweld Software. Journal of Polymer & Composites. 2023; 11(Special Issue 12): S101–S112.

the most critical factor is pin height and process pitch to determine faying surface lift, and there is no significant effect of tool tilt angle [8, 9]. 7075 aluminum alloy is a high-strength material commonly used in aerospace and defense applications due to its excellent mechanical properties, including high strength and toughness. However, it can be challenging to weld due to its susceptibility to hot cracking and poor weldability with traditional welding methods [10–16]

Regarding welding 2024 aluminum alloy, it is also commonly used in aerospace applications due to its high strength and good fatigue resistance. However, 2024 aluminum is known to have poor weldability due to its high susceptibility to cracking during welding [12, 13].

While FSW is a viable option for welding 2024 aluminum and 7075 aluminums, it can still present challenges due to its tendency to form cracks during welding. Therefore, it is essential to carefully control the welding parameters, such as the tool rotation speed, traverse speed, and tilt angle, to ensure a high-quality weld with minimal cracking.

In this research paper, an endeavor is made to study the simulation of the FSW process for AA2024, AA7075, and pure copper. L9 array is used to weld AA2024 and AA7075 with pure copper. The thermal stress and peak temperature are studied with the help of ALTAIR Hyperweld software.

MATERIALS AND METHODS

Selection of Materials

In this research, dissimilar aluminum alloys 7075, 2024, and copper are selected to be welded by FSW to find optimized process parameters for the welded joint. Altair's HyperWeld 2019 CAE software simulates the friction stir welding of AA7075, AA2024, and pure copper. In automobile and aircraft industries, these aluminum alloys and pure copper are extensively utilized. It is observed from the literature that very few investigations have been done to find out the effect on peak temperature due to process parameters and geometric parameters. So, in this paper, an endeavor is made to recognize the impact of these parameters on the welded plates utilizing the Hyper Weld module. The specimens are selected with a plate size of 300 mm*100 mm*6 mm [17]. The mechanical properties of the materials and tool are displayed in Tables 1 and 2, respectively.

Selection of Tool

H-13 steel tool pin is used to weld the plates. The tool geometry is cylindrical in shape having pin diameter (d = 5.5 mm), pin height (h = 5.4 mm), shoulder diameter (D = 18 mm), and shoulder length (L = 70 mm) as shown in Figures 1(a) and 1(b) represented how the dimension of the plate and tool specifications is entered in the software. Many researcher had been used H-13 steel as a tool material [14], [18–25].

Table 1. Aluminum alloy and Copper material properties.

Material	**AA 2024**	**AA 7075**	**Copper**
Density ('ρ' in Kg/m^3)	2780	2810	2700
Specific Heat ('Cp' in J/Kg-K)	827	960	900
Poisson Ratio(μ)	0.35	0.35	0.35
Co-efficient of Thermal Expansion (1/K)	1*10^(-5)	1*10^(-5)	1*10^(-5)
Young Modulus ('E' in N/m^2)	4.00*10^10	4.00*10^10	4.00*10^10
Solidus Temp (˚K)	775	750	889
Liquidus Temp (˚K)	911	908	927
Conductivity ('K' in W/m-K)	193	173	198

Table 2. H-13 Tool material properties.

Tool Material	**Density ('ρ' in Kg/m^3)**	**Specific Heat ('Cp' in J/Kg-K)**	**Conductivity ('K' in W/m-K)**	**Young Modulus ('E' in N/m^2)**	**Poisson Ratio**

H-13	7870	460	24.3	2.1*10^11	0.35

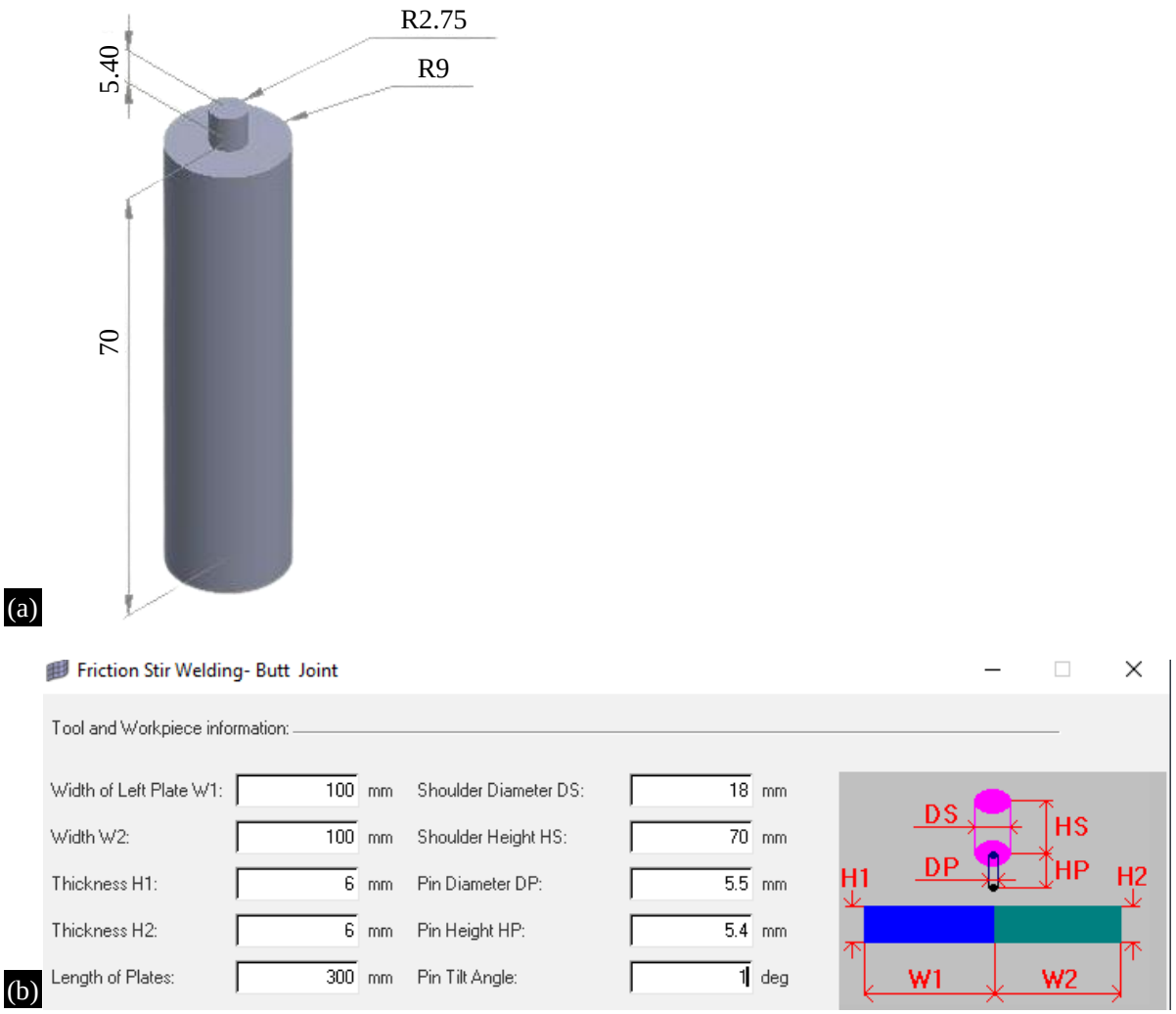

Figure 1. (a) Tool geometry, (b) Tool and workpiece data.

Table 3. Input Process parameters values and their levels.

Level	**A**	**B**	**C**
	Rotational speed (r.p.m)	***Welding speed (mm/s)***	***Tool tilt angle(degree)***
Level 1	500	0.1	1
Level 2	1000	0.2	2
Level 3	1500	0.3	3

EXPERIMENTAL DESIGN USING TAGUCHI METHOD

In this research, plates of 6 mm thickness of AA 2024 and AA 7075 is friction stir butt welded with pure copper using Hyper-weld software of Altair's. In this investigation rotational speed (R.P.M), welding speed (W.S), and tilt angle are taken as process parameters with three levels. The values of the parameters and their symbol were listed in Table 3.

Rotational speed, welding speed, and tool tilt angle are selected with three levels for L9 orthogonal design. Firstly, AA2024 and copper are welded together, with AA2024 placed on the retreating side and copper plate on the advance side. This research considers the effects of process parameters, not the interactions between them. Nine experiments were done to measure maximum temperature and residual stresses during the welding. Then, AA 2024 and copper are welded together, with AA 2024

placed on the left side and the copper plate on the right. *Similarly, AA 7075 and copper are welded* together. The virtual experiments are performed on different combinations of processed parameters, as shown in Figure 2. The initial temperature of the plate is taken as 30˚C, and the handle, top surface, and bench convection coefficient are taken as 7,14 and 210 W/m^2-C, respectively.

RESULTS AND DISCUSSION

The present simulations have been done for welding AA 2024 and AA 7075 with copper with three levels of different input parameters. Table 4 represented the maximum temperature and residual stresses simulated during the welding of AA 2024 and copper when AA 2024 is placed on the left side and copper plate on the right side. Signal to noise ratio is also calculated concerning temperature and stress for all sets.

It is observed from the Table 4 maximum temperature = 852.7 ˚ C and minimum residual stress = 14.22 MPa is simulated with experiment no. 7 (RPM = 1500, W.S = 0.1 mm/s and tool tilt angle = 3˚). And minimum temperature = 533.7 ˚ C and maximum residual stress 29.8 MPa is simulated with experiment no. 1 (RPM = 500, W.S = 0.1 mm/s and tool tilt angle = 1˚)

It is clear from Table 5 and Table 6 that rotation speed has more impact on temperature concerning the other two parameters as the delta value of R.P.M is very large compared with others.

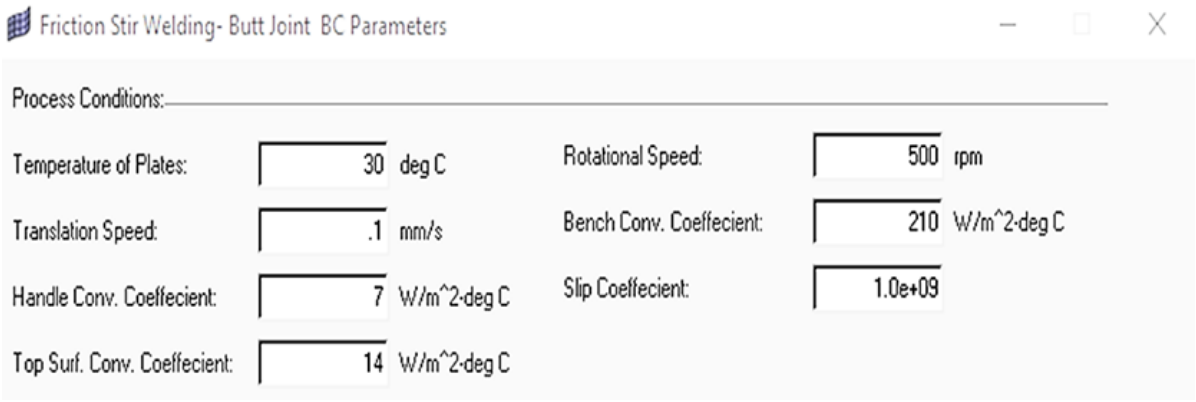

Figure 2. Process Parameter Information.

Table 4. Orthogonal array with S/N ratio when 2024 on the left side and copper on the right side.

	R.P.M	Welding speed (mm/s)	Tilt angle (dgree)	Temperature (°C)	S/N ratio (w.r.t temp.)	Stress (MPa)	S/N RATIO (w.r.t stress)
1	500	0.1	1	**533.7**	54.5459	**29.8**	-29.4872
2	500	0.2	2	535.9	54.5817	29.71	-29.4581
3	500	0.3	3	537.5	54.6076	21.69	-29.9827
4	1000	0.1	2	722.8	57.1816	17.45	-24.8359
5	1000	0.2	3	722.9	57.1828	18.54	-25.3622
6	1000	0.3	1	696.6	56.8597	19.11	-25.6252
7	1500	0.1	3	**852.7**	58.6169	**14.22**	-23.0580
8	1500	0.2	1	824.8	58.3291	14.48	-23.2094
9	1500	0.3	2	826.8	58.3480	14.27	-23.0885

Table 5. Signal to Noise Ratios for Larger is better.

Level	R.P.M	W.S	Tilt angle
1	54.58	56.78	56.58
2	57.07	56.70	56.70
3	58.43	56.61	56.80

Delta	3.85	0.18	0.22
Rank	1	3	2

Table 6. Signal to Noise Ratios for Smaller is better.

Level	R.P.M	W.S	Tilt angle
1	-29.64	-25.79	-26.11
2	-25.27	-26.01	-25.79
3	-23.12	-26.23	-26.13
Delta	6.52	0.44	0.34
Rank	1	2	3

Al on the left side, minimum temperature and stress profile

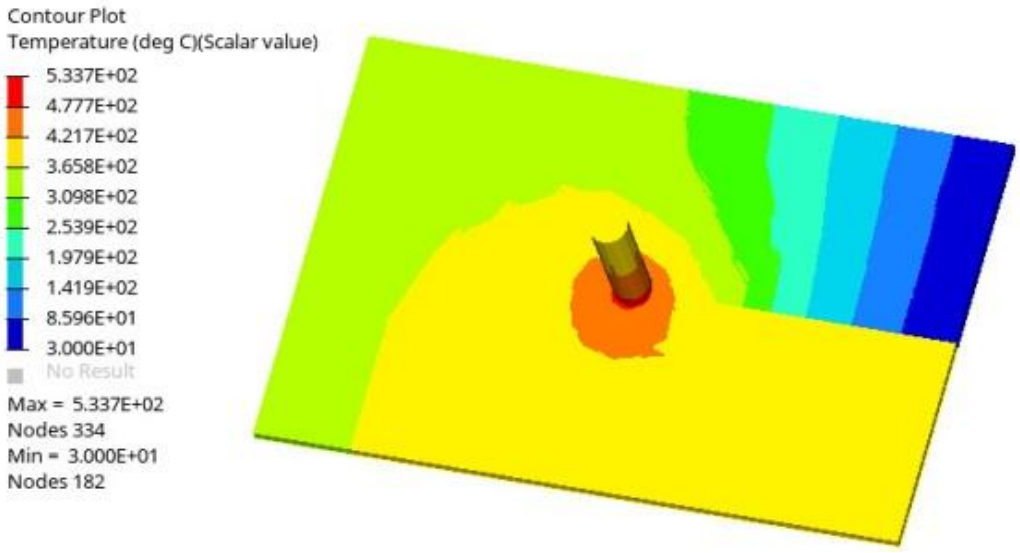

(a)

Al on the left, side maximum temperature and stress profile

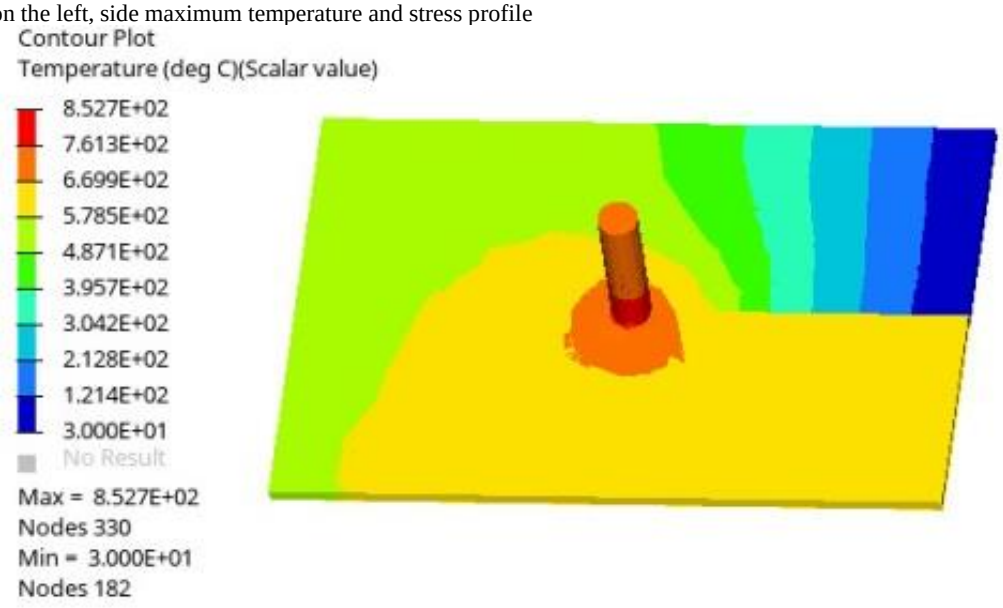

(b)

Al on the left side, minimum temperature and stress profile

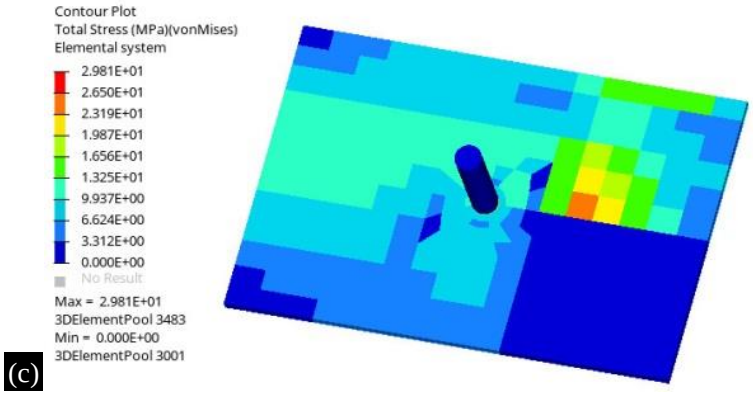

Al on the left, side maximum temperature and stress profile

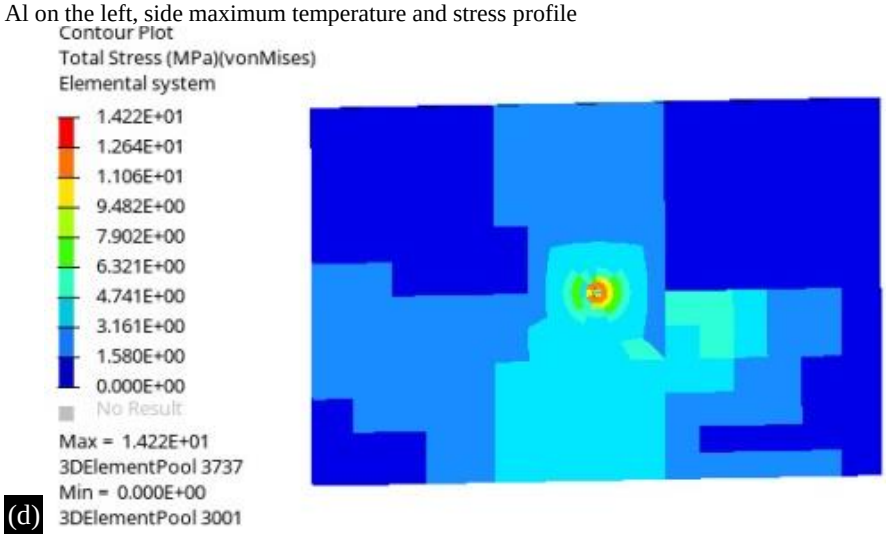

Figure 3. Temperature and Stress profile of AA2024 and Copper weld.

Table 7. Orthogonal array with S/N ratio when 2024 on the right side and copper on the left side.

	R.P.M	Welding speed (mm/s)	Tilt angle (dgree)	Temperature ($°C$)	S/N RATIO(w.r.t temp.)	Stress (MPa)	S/N RATIO (w.r.t stress)
1	500	0.1	1	**849.8**	58.5863	159.91	-35.5500
2	500	0.2	2	1219	61.7201	16.74	-24.4751
3	500	0.3	3	**1229**	61.7910	**16.09**	-24.1311
4	1000	0.1	2	924.4	59.3172	110.0	-40.8279
5	1000	0.2	3	916.8	59.2455	121.9	-41.7201
6	1000	0.3	1	903.4	59.1176	114.2	-41.1533
7	1500	0.1	3	1132	61.0769	63.05	-35.9937
8	1500	0.2	1	1126	61.0308	58.02	-35.2716
9	1500	0.3	2	1101	60.8357	65.53	-36.3288

Figure 3 represented the maximum temperature and residual stresses simulated during the welding of AA 2024 and copper when AA 2024 is placed on the left side and copper plate on the right side.

It is observed from Table 7, maximum temperature = 1229°C and minimum residual stress = 16.09 MPa is simulated with experiment no. 3, and minimum temperature = 849.8°C and maximum residual stress 159.91 MPa is simulated with experiment no. 1.

It is clear from Table 8 and Table 9 that rotation speed has more impact on temperature concerning

the other two parameters as the delta value of R.P.M is very large compared with others.

Table 8. Signal to Noise Ratios for Larger is better.

Level	R.P.M	W.S	Tilt angle
1	60.70	59.66	59.58
2	59.23	60.67	60.62
3	60.98	60.58	60.70
Delta	1.75	1.01	1.13
Rank	1	3	2

Table 9. Signal to Noise Ratios for smaller is better.

Level		R.P.M	W.S	Tilt angle
1		-28.05	-37.46	-37.32
2		-41.23	-33.82	-33.88
3		-35.86	-33.87	-33.95
Delta		13.18	3.63	3.45
Rank		1	2	3

Al on the right side, minimum temperature and stress profile

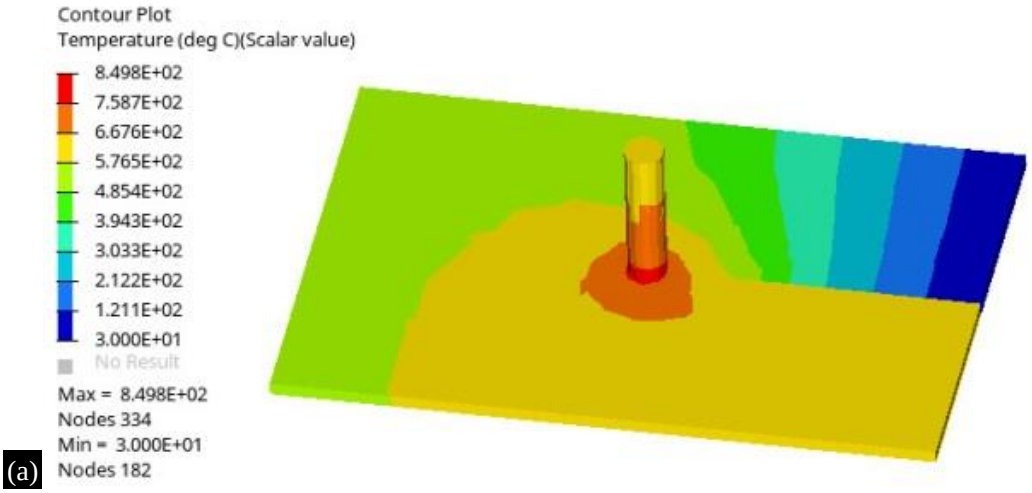

(a)

Al on the right, side maximum temperature and stress profile

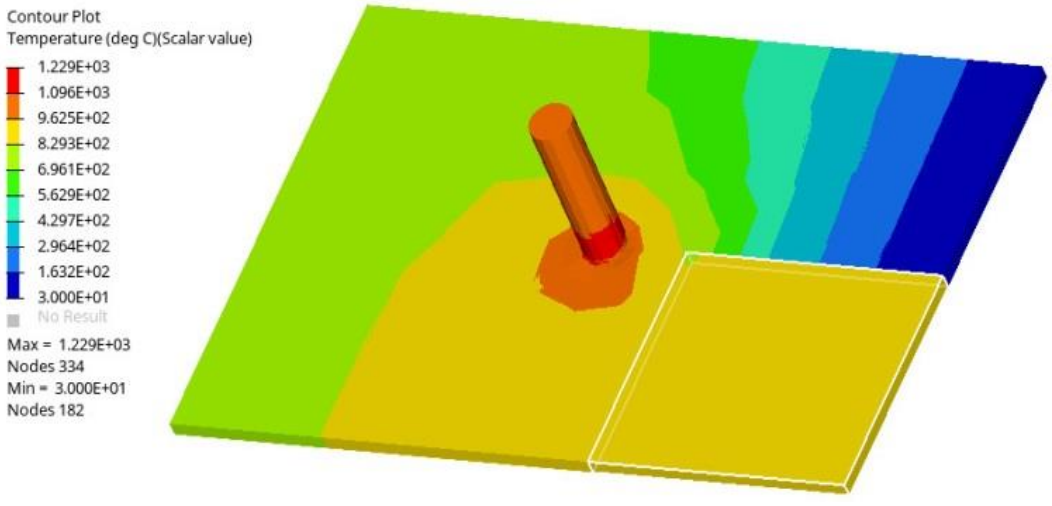

(b)

Al on the right side, minimum temperature and stress profile

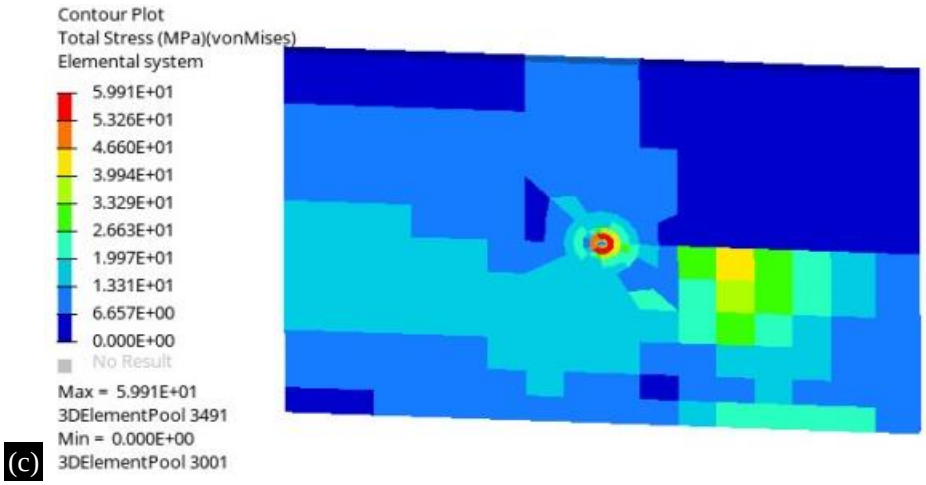

(c)

Al on the right, side maximum temperature and stress profile

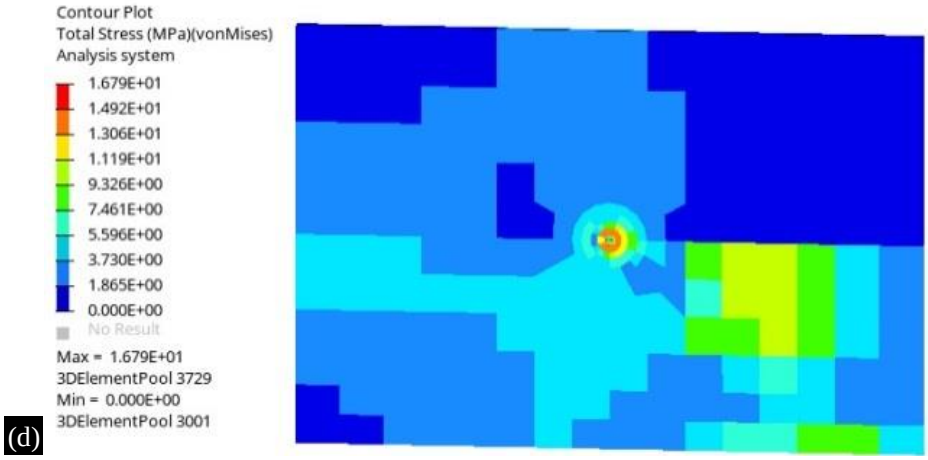

(d)

Figure 4. Temperature and Stress profile of AA2024 and Copper weld.

It is observed from the Table 10 maximum temperature = 1262 ˚ C and minimum residual stress = 24.70 MPa is simulated with experiment no. 7 (R.P.M = 1500, W.S = 0.1 mm/s and tool tilt angle = 3˚). And minimum temperature = 793.8 ˚ C is simulated with experiment no. 1 (R.P.M = 500, W.S = 0.1 mm/s and tool tilt angle = 1˚), but maximum residual stress 44.03 MPa is simulated with experiment no. 3 (R.P.M = 500, W.S = 0.3 mm/s and tool tilt angle = 3˚).

Table 10. Orthogonal array with S/N ratio when 7075 on the right side and copper on the left side.

R.P.M	Welding speed (mm/s)	Tilt angle (dgree)	Temperature (°C)	S/N RATIO (w.r.t temp.)	Stress (MPa)	S/N RATIO (w.r.t stress)
500	0.1	1	793.4	57.9898	41.37	-32.3337
500	0.2	2	794.6	58.0030	41.43	-32.3463
500	0.3	3	794.7	58.0041	44.03	-32.8750
1000	0.1	2	1061	60.5143	27.99	-28.9401
1000	0.2	3	1052	60.4403	30.60	-29.7144
1000	0.3	1	1029	60.2483	29.55	-29.4111
1500	0.1	3	**1262**	62.0212	**24.70**	-27.3247
1500	0.2	1	1247	61.9173	23.24	-27.8539
1500	0.3	2	1227	61.7769	23.85	-27.5498

It is clear from Table 11 and Table 12 that rotation speed has more impact on temperature

concerning the other two parameters as the delta value of R.P.M is very large compared with others.

Table 11. Signal to Noise Ratios for Larger is better.

Level	R.P.M	W.S	Tilt angle
1	58.00	60.18	60.05
2	60.40	60.12	60.10
3	61.91	60.01	60.16
Delta	3.91	0.17	0.10
Rank	1	2	3

Table 12. Signal to Noise Ratios for smaller is better.

Level	R.P.M	W.S	Tilt angle
1	-32.52	-29.71	-29.69
2	-29.36	-29.80	-29.61
3	-27.58	-29.95	-30.15
Delta	4.94	0.24	0.54
Rank	1	3	2

Al on the right side, minimum temperature and stress profile

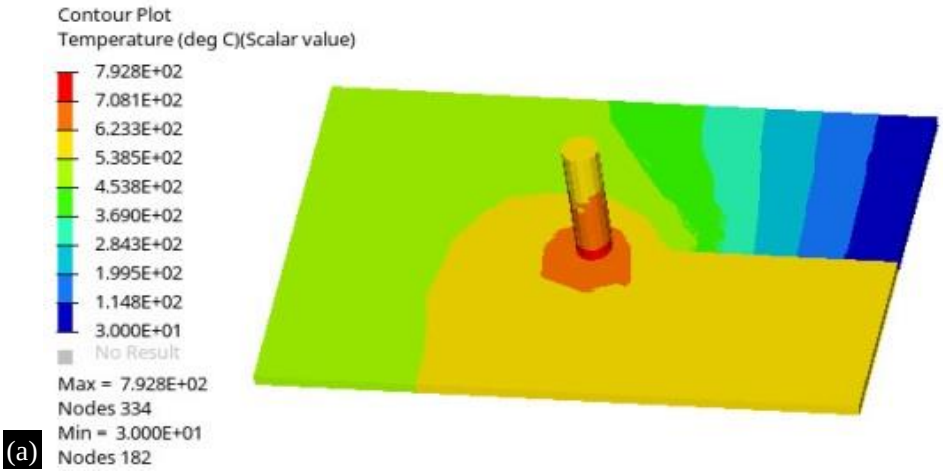

(a)

Al on the right, side maximum temperature and stress profile

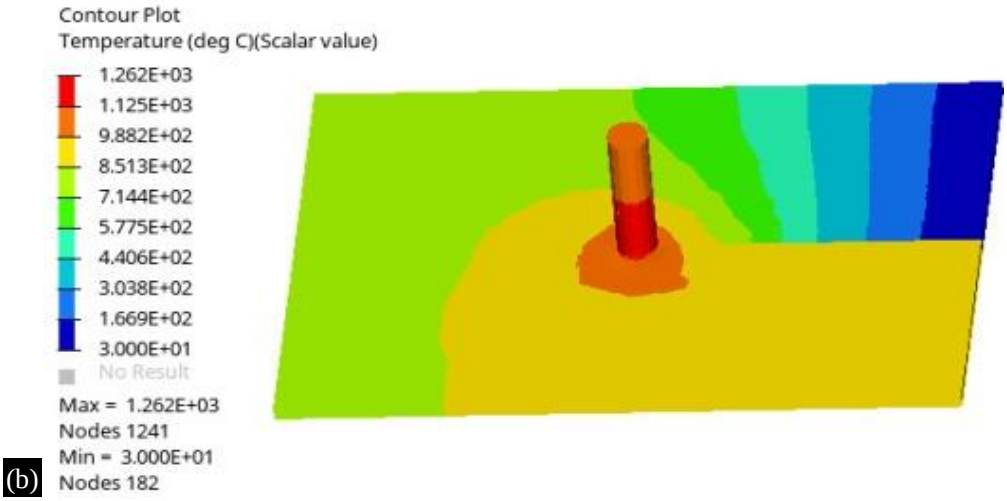

(b)

Al on the right side, minimum temperature and stress profile

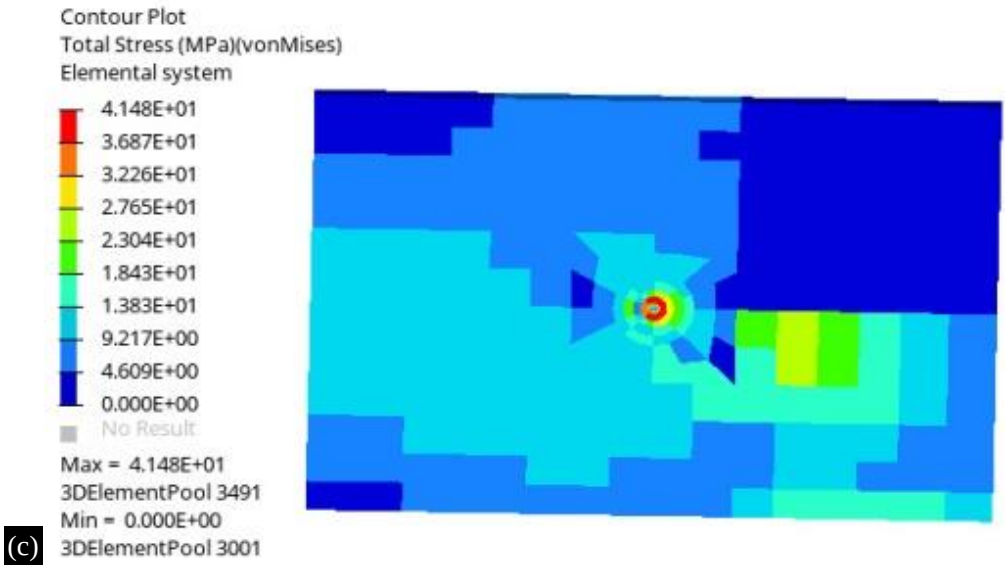

Al on the right, side maximum temperature and stress profile

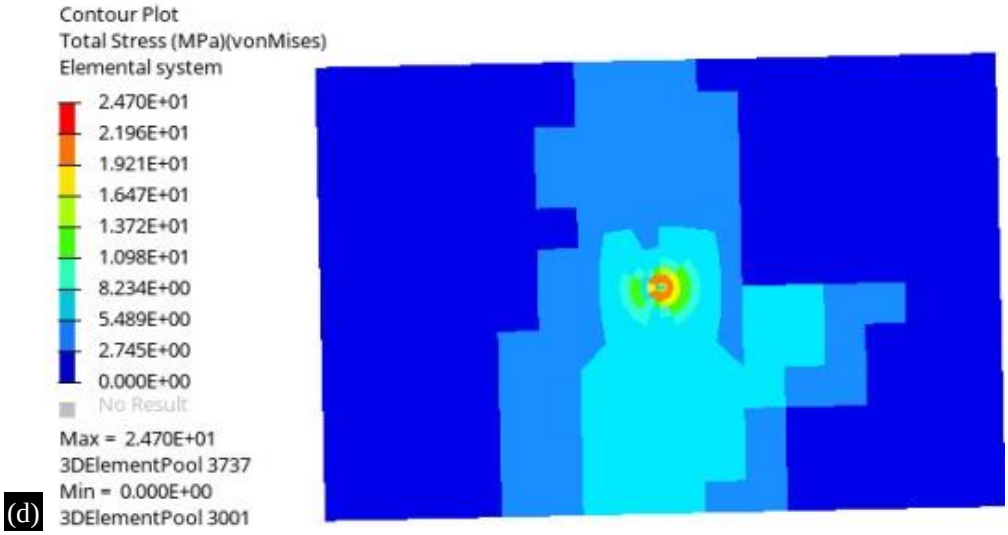

Figure 5. Temperature and Stress profile of AA7075 and Copper weld.

Figure 4 & 5 represented the maximum temperature and residual stresses simulated during the welding of AA 7075 and copper when AA 7075 is placed on the left side and copper plate on the right side. It is observed from all experiments that more temperature is generated when copper plate put on left side.

CONCLUSIONS

FSW reenactments are performed on Altair's HyperWeld to simulate the maximum temperature and minimum residual stresses.The following conclusions are predicted after the investigation:

- Maximum temperature and minimum residual stress are observed as 852.7˚ C and 14.22 MPa, respectively, during the FSW of AA2024 and copper when A.A. 2024 on the left side in experiment number 7.
- Maximum temperature and minimum residual stress are observed as 1229˚ C and 16.04 MPa during the FSW of AA2024 and copper when A.A. 2024 right plate with process parameter R.P.M. = 500, W.S. = 0.3 mm/s and tool tilt angle = 3˚,

- More heat is generated when the copper plate is placed on the left side.
- Maximum temperature and minimum residual stress are observed as 1262˚ C and 24.70 MPa, respectively, during the FSW of AA7075 and copper when AA7075 right plate with process parameter R.P.M. = 1500, tool tilt angle = 3˚and W.S. = 0.1 mm/s.
- Tool rotational speed significantly affects temperature rise during the friction stir welding of AA2074 and AA7075 with copper concerning the other two parameters.

REFERENCES

1. G. B. P. (December 1991). W.M. Thomas, E.D. Nicholas, J.C. Needham, M.G. Murch, P. Templesmith, C.J. Dawes, "No Title," Application No. 9125978.8
2. Satpute M. A., Patil S. S., Andhale S. R., and Gogte C. L., "Thermomechanical Modeling of Friction Stir Welding for Different Material using Altair's HyperWeld FSW," *Int. J. Eng. Res.*, vol. V4, no. 12, 2015, doi: 10.17577/ijertv4is120001.
3. Husain Mehdi, R.S. Mishra, Investigation of mechanical properties and heat transfer of welded joint of AA6061 and AA7075 using TIG+FSP welding approach, Journal of Advanced Joining Processes, 1, 100003, (2020) https://doi.org/10.1016/j.jajp.2020.100003.
4. Husain Mehdi, R.S. Mishra, Effect of Friction Stir Processing on Microstructure and Mechanical Properties of TIG Welded Joint of AA6061 and AA7075, Metallography, Microstructure, and Analysis, 9, 403–418 (2020). https://doi.org/10.1007/s13632-020-00640-7
5. Husain Mehdi, R.S. Mishra, Effect of friction stir processing on mechanical properties and heat transfer of TIG welded joint of AA6061 and AA7075, Defence Technology, 17 (3), 715-727 (2021). https://doi.org/10.1016/j.dt.2020.04.014
6. Husain Mehdi, R.S. Mishra, Influence of Friction Stir Processing on Weld Temperature Distribution and Mechanical Properties of TIG-Welded Joint of AA6061 and AA7075. Transactions of the Indian Institute of Metals, 73, 1773–1788 (2020). https://doi.org/10.1007/s12666-020-01994-w
7. Husain Mehdi, R.S. Mishra, an experimental analysis and optimization of process parameters of AA6061 and AA7075 welded joint by TIG+FSP welding using RSM, Advances in Materials and Processing Technologies, 8(1), 598–620, 2022. https://doi.org/10.1080/2374068X.2020.1829952.
8. M. K. Yadava, R. S. Mishra, Y. L. Chen, B. Carlson, and G. J. Grant, "Study of friction stir joining of thin aluminium sheets in lap joint configuration," vol. 15, no. 1, pp. 70–76, 2010, doi: 10.1179/136217109X12537145658733.
9. R. S. Mishra and Z. Y. Ma, "Friction stir welding and processing," vol. 50, pp. 1–78, 2005, doi: 10.1016/j.mser.2005.07.001.
10. H. Akkus, "Determining the effect of cutting parameters on surface roughness in hard turning using the Taguchi method," vol. 44, pp. 1697–1704, 2011, doi: 10.1016/j.measurement.2011.07.003.
11. J. M. Piccini and H. G. Svoboda, "Tool geometry optimization in friction stir spot welding of Al-steel joints," *J. Manuf. Process.*, vol. 26, pp. 142–154, 2017, doi: 10.1016/j.jmapro.2017.02.004.
12. M. M. Moradi, H. J. Aval, and R. Jamaati, "Microstructure and mechanical properties in nano and microscale SiC-included dissimilar friction stir welding of AA6061-AA2024," vol. 0836, no. November, 2017, doi: 10.1080/02670836.2017.1393976.
13. H. Ji, Y. Deng, H. Xu, S. Lin, W. Wang, and H. Dong, "The mechanism of rotational and non-rotational shoulder affecting the microstructure and mechanical properties of Al-Mg-Si alloy friction stir welded joint," *Mater. Des.*, vol. 192, p. 108729, 2020, doi: 10.1016/j.matdes.2020.108729.
14. S. Sinhmar and D. K. Dwivedi, "Effect of weld thermal cycle on metallurgical and corrosion behavior of friction stir weld joint of AA2014 aluminium alloy," *J. Manuf. Process.*, vol. 37, no. July 2018, pp. 305–320, 2019, doi: 10.1016/j.jmapro.2018.12.001.
15. "Effect of Tool Geometry on Mechanical and Micro-structural properties of Friction Stir Welding of Al-alloy," no. 2007, pp. 88–92, 2014.
16. S. W. Kallee, *Industrial applications of friction stir welding*. Woodhead Publishing Limited, 2009. doi: 10.1533/9781845697716.1.118.

17. A. O. Al-Roubaiy, S. M. Nabat, and A. D. L. Batako, "Experimental and theoretical analysis of friction stir welding of Al–Cu joints," *Int. J. Adv. Manuf. Technol.*, vol. 71, no. 9–12, pp. 1631–1642, 2014, doi: 10.1007/s00170-013-5563-z.
18. L. Fratini and G. Buffa, "CDRX modelling in friction stir welding of aluminium alloys," vol. 45, pp. 1188–1194, 2005, doi: 10.1016/j.ijmachtools.2004.12.001.
19. R. Beygi, M. Kazeminezhad, and A. H. Kokabi, "Microstructural Evolution and Fracture Behavior of Friction-Stir-Welded Al-Cu Laminated Composites," vol. 45, no. January, pp. 361–370, 2014, doi: 10.1007/s11661-013-1989-z.
20. E. T. Akinlabi, "Effect of shoulder size on weld properties of dissimilar metal friction stir welds," *J. Mater. Eng. Perform.*, vol. 21, no. 7, pp. 1514–1519, 2012, doi: 10.1007/s11665-011-0046-6.
21. Galvão, A. Loureiro, D. Verdera, D. Gesto, and D. M. Rodrigues, "Influence of tool offsetting on the structure and morphology of dissimilar aluminum to copper friction-stir welds," *Metall. Mater. Trans. A Phys. Metall. Mater. Sci.*, vol. 43, no. 13, pp. 5096–5105, 2012, doi: 10.1007/s11661-012-1351-x.
22. K. S. Mehra and S. Singh, "Investigation of Friction stir welded joint of AA6061 material using Altair Hyper Weld," vol. 7, no. 12, pp. 305–309, 2016.
23. R. Butola, Q. Murtaza, and R. M. Singari, "An experimental and simulation validation of residual stress measurement for manufacturing of friction stir processing tool," *Indian J. Eng. Mater. Sci.*, vol. 27, no. 4, pp. 826–836, 2020.
24. R. Butola, N. Choudhary, R. Kumar, P. Kumar, M. Zubair, and R. M. Singari, "Materials Today : Proceedings Measurement of residual stress on H13 tool steel during machining for fabrication of FSW / FSP tool pins," *Mater. Today Proc.*, no. xxxx, 2020, doi: 10.1016/j.matpr.2020.11.656.
25. V. J. Arulmoni, R. S. Mishra, and M. S. Ranganath, "Experimental Investigations on Friction Stir Processed Copper and Enhancement of Mechanical Properties of the Composite Material Experimental Investigations on Friction Stir Processed Copper and Enhancement of Mechanical Properties of the Composite Materi," no. September, 2014.

